

MODELING FLARES PRODUCED IN BLAZARS

Marek Sikora¹, Michał Błażejowski¹, Greg Madejski², and Rafał Moderski³

¹Nicolaus Copernicus Astronomical Center, Warsaw

²Stanford Linear Accelerator Center, Menlo Park, CA 94025, USA

³JILA, University of Colorado, Boulder, CO

ABSTRACT

We model light curves of flares observed in blazars, assuming that they are produced by relativistic electrons/positrons injected by forward-reverse shocks traveling down the jet with relativistic speeds. We approximate the radiating region as a thin shell enclosed between the two shock fronts. In addition to the conventional radiation processes such as synchrotron radiation and its Comptonization, we take into account Comptonization of light originating in the broad emission line region, and Comptonization of IR radiation from hot dust. We demonstrate that flares produced in the adiabatic regime decay much slower than flares produced in the radiative regime. The lack of such a difference between the X-ray and γ -ray flares in 3C279 strongly supports the synchrotron-self Compton (SSC) mechanism as responsible for X-ray production in this object. Finally, we discuss a possible scenario which can explain the ‘cooling’ nature of the MeV peak in blazars by comparing the flares produced in soft γ -ray band and above 100 MeV.

Key words: Blazars; γ -rays; flares.

1. THE MODEL

In our model we adopt the shock-in-jet scenario, in which individual flares are produced by shocks formed due to velocity irregularities in the beam and traveling down the jet with relativistic speeds.

The model assumptions are as follows:

- non-thermal plasma producing flares is enclosed within thin shells, each with a radial comoving width, λ' , much smaller than its cross-sectional radius a ;
- shells propagate down the conical jet with a constant Lorentz factor Γ ;

- magnetic fields, carried by the beam, scale with distance as $B' \propto 1/r$;
- both magnetic field intensity and particle distribution are uniform across the shell;
- relativistic electrons/positrons are injected into the shell within a finite distance range Δr_{inj} and with injection starting at r_0 , at a rate parameterized by $Q = K\gamma^{-p}$ for $\gamma_m < \gamma < \gamma_{max}$, and $Q \propto \gamma^{-1}$ for $\gamma < \gamma_m$, where γ is the random Lorentz factor of an electron/positron;
- radiative energy losses of relativistic electrons/positrons are dominated by three processes: external-radiation Comptonization (ERC):

$$\left(\frac{d\gamma}{dt'}\right)_{ERC} = -\frac{16\sigma_T}{9m_e c}(u_{BEL} + u_{IR})\Gamma^2\gamma^2, \quad (1)$$

synchrotron radiation :

$$\left(\frac{d\gamma}{dt'}\right)_{SYN} = -\frac{4\sigma_T}{3m_e c}u'_B\gamma^2, \quad (2)$$

and Comptonization of synchrotron radiation :

$$\left(\frac{d\gamma}{dt'}\right)_{SSC} = -\frac{4\sigma_T}{3m_e c}u'_S\gamma^2, \quad (3)$$

where $u'_B = B'^2/8\pi$ is the magnetic field energy density, u'_S is the energy density of the synchrotron radiation field, $u_{BEL} \simeq (\partial L_{BEL}/\partial \ln r)/4\pi r^2 c$ is the energy density of the broad emission line field at the actual distance of a source/shell propagating downstream a jet, $u_{IR} \simeq \xi_{IR} 4\sigma_{SB} T^4/c$ is the energy density of the infrared radiation field, ξ_{IR} is the fraction of the central radiation reprocessed into near infrared by dust, and T is the temperature of dust.

- the observer is located at an angle $\theta_{obs} = 1/\Gamma$ from the jet axis.

- evolution of electrons is described by a continuity equation (Moderski et al. 2000; Błażejowski et al. 2000)

$$\frac{\partial N_\gamma}{\partial r} = -\frac{\partial}{\partial \gamma} \left(N_\gamma \frac{d\gamma}{dr} \right) + \frac{Q}{c\beta\Gamma}, \quad (4)$$

where the rate of electron/positron energy losses is

$$\frac{d\gamma}{dr} = \frac{1}{\beta c\Gamma} \left(\frac{d\gamma}{dt'} \right)_{rad} - \frac{\gamma}{r}, \quad (5)$$

$\beta = \sqrt{\Gamma^2 - 1}/\Gamma$, and $dr = \beta c\Gamma dt'$. The second term on the right-hand side of eq. (5) represents the adiabatic energy losses.

2. ADIABATIC VS. RADIATIVE LOSSES

Here we compare the time profiles of flares produced by electrons radiating their energy in adiabatic ($\gamma \ll \gamma_c$) and radiative ($\gamma \gg \gamma_c$) regimes, where γ_c is the energy of electrons for which the radiative cooling time scale is equal to the injection time scale. Presented flares are produced by the ERC process and all computations are made under assumption that this process strongly dominates the entire radiative losses. A comparison of two profiles in Fig. 1 illustrates that adiabatic flares decay much more slowly than radiative ones. This property of flares produced in the two regimes can be used to verify X-ray production mechanisms in blazars (see next section).

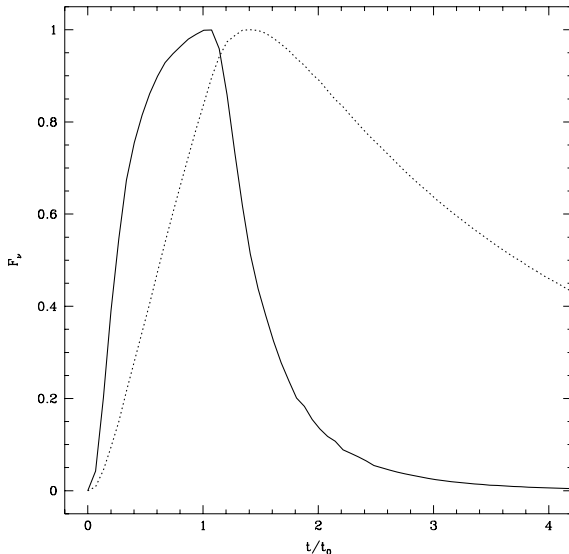


Figure 1. Adiabatic (dotted line) vs. radiative (solid line) flares. Note that $t_0 = r_0/(1 + \beta)\beta c\Gamma^2 \approx r_0/2c\Gamma^2$.

3. CONFRONTATION WITH OBSERVATIONS - 3C 279

3C 279 is among the best monitored blazars over a broad range of energies. In this section we use the simultaneous multi-wavelength observations carried out in February 1996 (Wehrle et al. 1998) to infer about the radiative processes operating in this object. The most interesting result of this campaign was the very close correspondence between the X-ray and γ -ray light curves during the outburst. There was no evidence of any significant time lag between the peaks; furthermore, both curves decayed at the same rate. The above facts suggest the following scenario: X-rays are produced via SSC the process and γ -rays by ERC (see Fig. 2 for details). We can definitely exclude a model where both energy bands are produced by the ERC process alone. This is due to the fact that the production of X-rays by ERC involves low energy electrons, which radiate in the adiabatic regime. As was shown in previous section, adiabatic flares decay much more slowly than radiative ones. Thus, the observed γ -ray – X-ray correlation excludes the production of X-rays by the ERC process, unless the decay rate is determined by the deceleration of the shell and/or a change in its direction of motion.

4. THE MEV BREAK-PREDICTIONS VS. OBSERVATIONS

In previous sections it was assumed that the break in the electron injection function, γ_m , is located at lower energies than the break caused by inefficient radiative cooling of electrons with $\gamma < \gamma_c$. With this assumption, the characteristic break of the high energy spectra in the 1–30 MeV range is related to the break of the electron energy distribution at γ_c . As was discussed by Sikora (1997), such an interpretation of the MeV break is consistent with the observed flare time scales. Assuming that the distance of flare production is of the order $r_{fl} \sim ct_{fl}\Gamma^2$, one can find that flares lasting \sim days are produced at distances $10^{17} - 10^{18}$ cm, and that at such distances ERC radiation is inefficient at $h\nu < 1 - 30$ MeV.

However, the time resolution of recent high-energy experiments is not good enough to reject the possibility that the observed flares are superpositions of several shorter-lasting flares, which are produced much closer to the central engine than the ~ 1 -day variability time scales may suggest. Due to the stronger magnetic and external radiation fields at smaller distances, the value of γ_c would be lower and the break would appear at $h\nu \ll 1$ MeV. In order to explain the observed MeV breaks, one would then have to assume that this break is related to the break in the electron injection function. There are two ways to distinguish between these possibilities, either by studying spectral slopes, or by studying flare profiles, both below and above the MeV break. The first approach is based on the fact that for $\gamma_m < \gamma_c$,

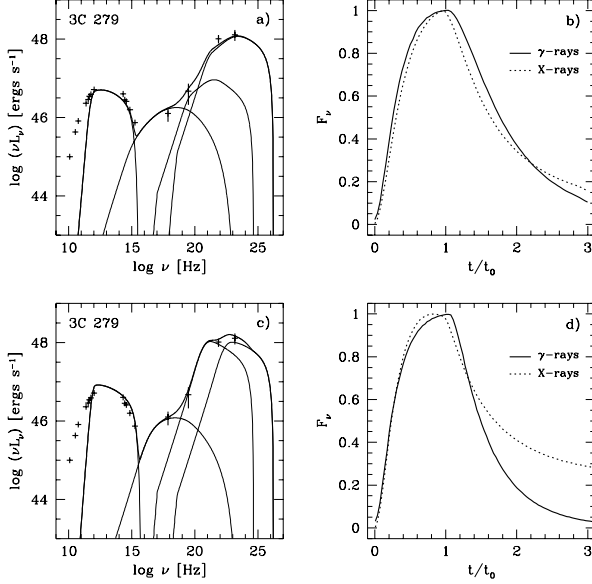


Figure 2. Modeling the Feb-96 event in 3C 279. Left panels: two model fits to the time averaged outburst spectrum. All observational data are simultaneous and taken from Wehrle et al. (1998). Right panels: model γ -ray flare, with the flux integrated over energies > 100 MeV, vs. model X-ray flare, with the flux taken at 2 keV. The upper panels are for the model with parameters: $\Gamma = 20$; $r_0 = 6.0 \times 10^{17}$ cm; $\Delta r_{inj}/r_0 = 1$; $Q = \text{const}$, with $\gamma_m = 27$, $\gamma_{max} = 6.5 \times 10^3$ and $p = 2.4$, and electron injection luminosity $L_e = 1.6 \times 10^{44}$ ergs s $^{-1}$; $B' = 0.53(r_0/r)$ Gauss; and energy densities of the ambient diffuse radiation field s , $u_{BEL} = 4.9 \times 10^{-4}(r_0/r)^2$ ergs cm $^{-3}$ and $u_{IR} = 1.0 \times 10^{-5}$ ergs cm $^{-3}$. The lower panels are for the model with parameters: $\Gamma = 20$; $r_0 = 7.0 \times 10^{17}$ cm; $\Delta r_{inj}/r_0 = 1$; $Q = \text{const}$, with $\gamma_m = 150$, $\gamma_{max} = 6.5 \times 10^3$ and $p = 2.4$, and $L_e = 0.6 \times 10^{44}$ ergs s $^{-1}$; $B' = 0.81(r_0/r)$ Gauss; and energy densities of the ambient diffuse radiation field s , $u_{BEL} = 5.9 \times 10^{-4}(r_0/r)^2$ ergs cm $^{-3}$ and $u_{IR} = 2.0 \times 10^{-4}$ ergs cm $^{-3}$.

the slope of the radiation spectrum produced by electrons with $\gamma_m \ll \gamma \ll \gamma_c$ should be harder by $\delta\alpha = 0.5$ than the slope of the radiation spectrum produced by electrons with $\gamma \gg \gamma_c$. But in the case $\gamma_c < \gamma_m$, the slope of the radiation spectrum produced by electrons with $\gamma_c \ll \gamma \ll \gamma_m$ is predicted to be $\alpha = 0.5$, independent of the spectral slope produced at $\nu \gg \nu(\gamma_m)$ (see, e.g., Sari, Piran & Narayan 1998). The second approach, proposed in this paper, uses the fact that adiabatic flares decay much more slowly than radiative ones (see Fig. 2). Thus, in the case $\gamma_m < \gamma_c$, the flares observed in OVV/HP quasars at sub-MeV energies should decay much more slowly than in the case $\gamma_c < \gamma_m$. Our predictions are presented for the model, for which $u_{BEL} = \text{const}$. One can see that the higher the energy, the more rapidly the flare peaks (Fig. 3 – lower panels). Please note that this numerical result is

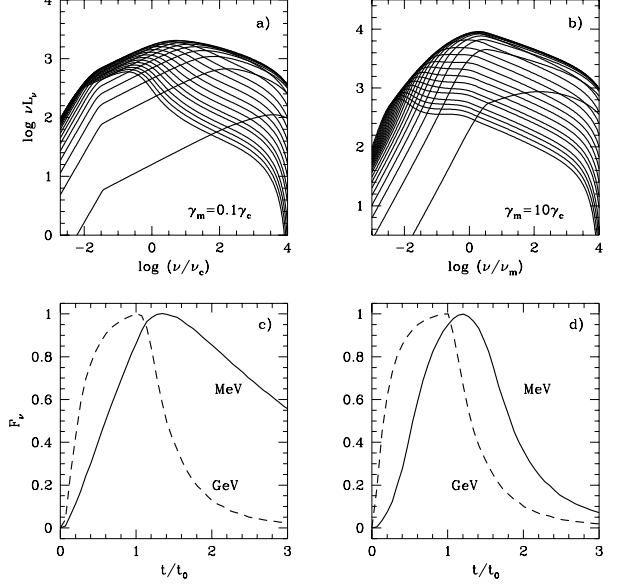


Figure 3. Variability around the ERC peak. Left panels are for the peak produced by electrons with energies $\gamma \sim \gamma_c$, while right panels are for the peak determined by electrons with $\gamma \sim \gamma_m$. The spectra are shown with a time step $\delta t/t_0 = 0.14$ and are followed up to $t = 3t_0$. The flares are shown at frequencies: (c) $\nu = 0.1\nu_c$ (solid line) and $\nu = 100\nu_c$ (dashed line), where $\nu_c = (16/9)\Gamma^2\gamma_c^2\nu_{IR}$, (ν_{IR} is the frequency of the Comptonized photon); (d) $\nu = 0.1\nu_m$ (solid line) and $\nu = 100\nu_m$ (dashed line), where $\nu_m = (16/9)\Gamma^2\gamma_m^2\nu_{IR}$. $(d\gamma/dt')_{ERC}$ is assumed to be distance independent.

qualitatively consistent with observations presented by Zhang et al. 2000 (these proceedings). These authors present simultaneous observations of flaring blazar PKS 1622-297 showing the pronounced time lag between flare detected by EGRET ($E > 100$ MeV) and COMPTEL (10-30 MeV). Observations indicate a time delay of about 4 days between the two bands.

REFERENCES

- Błażejowski, M., Sikora, M., Moderski, R., Madejski, G.M. 2000, ApJ 545, 107
- Moderski, R., Sikora, M., & Bulik, T. 2000, ApJ 529, 151
- Sari, R., Piran, T., & Naryan, R. 1998, ApJ 497, L17
- Sikora, M. 1997, AIP Conf. Proc. 410, 4th Compton Symp., ed. C.D. Dermer, M.S. Strickman, & J.D. Kurfess (Woodbury, NY: AIP) 410, 494
- Wehrle, A.E. et al., 1998, ApJ 497, 178
- Zhang, S. et al., 2000, poster 4.49